Novel Reactions of Iron(III) Tetraphenylporphyrin π-Cation Radicals with Pyridine

Krystyna Rachlewicz and Lechosław Latos-Grażyński*

Institute of Chemistry, University of Wrocław, 14 F. Joliot-Curie St., Wrocław 50 383, Poland

Received July 2, 1993[⊗]

The reactivity of iron(III) tetraphenylporphyrin π-cation radical complexes [(TPP•)$Fe^{III}Cl$][$SbCl_6$] (**1**-1) and [(TPP•)-$Fe^{III}(ClO_4)_2$] (**1**-2) with pyridine has been examined by ^1H and ^2H NMR spectroscopy in dichloromethane solution at low temperatures. Evidence for the reaction of the porphyrin ring with pyridine with formation of stable β-pyridiniumyltetraphenylporphyrin (**2**) and unstable 5-pyridiniumylisotetraphenylporphyrin (**3**) and 5,10-dipyridiniumyltetraphenylporphodimethene (**4**) complexes of iron is presented. Forms **3** and **4** may be directly observed over the temperature range −80 to −40 °C. They are new forms of highly oxidized, highly positively charged species that are related to the iron porphyrins. The characteristic patterns of paramagnetically shifted pyrrole resonances (*i.e.*, seven for the β-substituted form, four for isoporphyrin, and two for porphodimethene iron complexes) are correlated with the symmetry of species and have been used as a definitive indication of porphyrin structural modification. The simultaneous formation of pyridine-substituted iron porphyrins in different oxidation/electronic/spin states has been found. A mechanism of their formation, which involves meso- or β-substituted σ-intermediates, has been proposed. The ^1H NMR spectra of the stable, high-spin [(β-py-TPP)-$Fe^{III}Cl_2$ and low-spin [(β-py-TPP)$Fe^{III}(py)_2$]Cl_2 products are presented and analyzed. A strong dependency of the ^1H NMR spectra on the counteranion for the low-spin form ([(β-py-TPP)Fe^{III}]$^{2+}$) has been found and is explained by the formation of a tightly bonded, ionic pair because the complex bears two positive charges.

Introduction

Interest in the function, stabilization, and electronic and molecular structure of iron porphyrin π-cation radicals results from the crucial importance of high-valent intermediates in enzymatic cycles of hemoproteins (peroxidases, catalases, cytochrome P-450, cytochrome oxidase)[1,2] and in catalytic reactions of iron porphyrins.[3,4] Reversible one- or two-electron oxidations of iron(III) porphyrins to form ferryl porphyrins or ferryl porphyrin π-cation radicals, respectively, were established in the course of these studies. Considerable effort has been directed to elaborate the mechanism of the reactions where the highly oxidized porphyrins are generated in the activation and transfer of oxygen, particularly in catalytic epoxidation/hydroxylation processes.[3-8]

The same heme/dioxygen combination is used in nature to destroy unwanted heme via iron oxophlorin intermediates.[9-12] The catalytic reactions are frequently accompanied by catalyst degradation which results in the modification of the porphyrin. Highly oxidized forms of myoglobin react with thiols to form sulfmyoglobin with an insertion of sulfur at the β-pyrrole position(s).[13,14] Highly oxidized iron porphyrins react at the meso position, and this is related to the topology of the hemoprotein crevice.[15-18] The reaction of horse myoglobin with H_2O_2 results in covalent binding of the heme prosthetic group to the protein via tyrosine-103.[15,16] The meso addition of radicals to the prosthetic group of horseradish peroxidase was also determined.[17] Additionally alkylhydrazines produce meso-alkylation products when reacted with myoglobin.[18] The formation of N-substituted porphyrins via iron(IV) intermediates was demonstrated to be involved in the reactions of hemoproteins with exogenous substances.[19-22] Synthetic iron *meso*-tetraphenylporphyrins that are able to catalyze the oxidation of

⊗ Abstract published in *Advance ACS Abstracts,* January 1, 1995.

(1) Dawson, J. H. *Science* **1988**, *240*, 433.
(2) Dunford, H. B. In *Peroxidase in Chemistry and Biology*; Everse, J., Everse, K. E., Grisham, M. B., Eds.; CRC Press: Boca Raton, FL, 1991; Vol. II, p 1.
(3) McMurry, T. J.; Groves, J. T. In *Cytochrome P-450, Structure, Mechanism and Biochemistry*; Ortiz de Montellano, P. R., Ed.; Plenum Press: New York, 1986; p 1.
(4) Meunier, B. *Bull. Soc. Chim. Fr.* **1986**, 578.
(5) Arasasingham, R.; Balch, A. L.; Latos-Grażyński, L. *Studies in Organic Chemistry 33.* In *The Role of Oxygen in Chemistry and Biochemistry*; Ando, W.; Moro-Oka, Y., Eds., Elsevier: New York, 1988, p 417.
(6) Balch, A. L. *Inorg. Chim. Acta* **1992**, *198-200*, 297.
(7) Groves, T. J.; Watanabe, Y. *J. Am. Chem. Soc.* **1988**, *110*, 8443.
(8) Mansuy, D. *Pure Appl. Chem.* **1987**, *59*, 759.
(9) Bissell, D. M. In *Liver: Normal Function and Disease. Bile Pigments and Jaundice*; Ostrow, J. D., Ed.; Marcel Decker, Inc.: New York, 1986; Vol. 4, p 133.
(10) Schmidt, R.; McDonach, A. F. In *The Porphyrins*; Dolphin, D., Ed.; Academic Press: New York, 1979; Vol. 6, p 258.
(11) O'Cara, P. In *Porphyrins and Metalloporphyrins*; Smith, K. M., Ed.; Elsevier: New York, 1975; p 122.
(12) Balch, A. L.; Latos-Grażyński, L.; Noll, B. C.; Olmstead, M. M.; Zovinka, E. *Inorg. Chem.* **1992**, *31*, 2248.
(13) Andersson, L. A.; Loehr, M. T.; Lim, A. R. Mauk, A. G. *J. Biol. Chem.* **1984**, *259*, 15340.
(14) Chatfield, M. J.; La Mar, G. N.; Parker, W. O.; Smith, K. M.; Leung, H.-K.; Morris, I. K. *J. Am. Chem. Soc.* **1988**, *110*, 6352.
(15) Catalano, C. E.; Choe, Y. S.; Ortiz de Montellano, P. R. *J. Biol. Chem.* **1989**, *264*, 10534.
(16) Fox, J. B.; Nicholas, R. A.; Ackerman, S. A.; Swift, C. E. *Biochemistry* **1974**, *13*, 5178.
(17) (a) Ator, M. A.; Ortiz de Montellano, P. R. *J. Biol. Chem.* **1987**, *262*, 1542. (b) Ator, M. A.; David, S. K.; Ortiz de Montellano, P. R. *J. Biol. Chem.* **1987**, *262*, 14954. (c) Ortiz de Montellano, P. R. *Acc. Chem. Res.* **1987**, *20*, 289. (d) DePillis, G. D.; Ortiz de Montellano, P. R. *J. Cell. Biol.* **1989**, *107*, 619a.
(18) Choe, Y. S.; Ortiz de Montellano, P. R. *J. Biol. Chem.* **1991**, *266*, 8523.
(19) Lavallee, D. K. *The Chemistry and Biochemistry of N-substituted Porphyrins*; VCH Publishers: New York, 1987.
(20) (a) Swanson, B. A.; Ortiz de Montellano, P. R. *J. Am. Chem. Soc.* **1991**, *113*, 8146. (b) Reich, N. O.; Ortiz de Montellano, P. R. In *Cytochrome P-450, Structure, Mechanism and Biochemistry*; Ortiz de Montellano, P. R., Ed.; Plenum Press: New York, 1986; pp 273-514. (c) Delaforge, M.; Battioni, P.; Mahy, J. P.; Mansuy, D. *Chem. Biol. Interact.* **1986**, *60*, 101. (d) Raag, R.; Swanson, B. A.; Poulos, T. L.; Ortiz de Montellano, P. R. *Biochemistry* **1990**, *29*, 8119. (e) Ortiz de Monterllano, R. P.; Kerr, D. E. *J. Biol. Chem.* **1983**, *258*, 10558. (f) Ringe, D.; Petsko, G. A.; Kerr, D. E.; Ortiz de Montellano, P. R. *Biochemistry* **1984**, *23*, 2. (g) Augusto, O.; Kunze, K. L.; Ortiz de Montellano, P. R. *J. Biol. Chem.* **1982**, *257*, 6231.
(21) Jonen, H. G.; Werringloer, J.; Prough, R. A.; Estabrook, R. W. *J. Biol. Chem.* **1982**, *257*, 4404.

0020-1669/95/1334-0718$09.00/0

olefins with nonphysiological oxidants (iodosarenes or hypochlorite) also undergo N-alkylation during the catalytic cycle.[23-26]

It has been suggested that highly oxidized iron porphyrin complexes can generate iron porphyrin π-cation or protein radicals even if the oxidizing equivalent is initially present as Fe^{IV} or $Fe^{IV}O$ (ferryl).[27] Understanding of the elementary degradation steps for both biochemical and synthetic systems requires better knowledge of the π-cation radical nature of highly oxidized iron porphyrins. However, the reactivity of iron(III) porphyrin cation radical complexes at the porphyrin periphery has received relatively little study. Two distinct patterns of reactivity of the diperchlorate iron(III) tetraphenylporphyrin π-cation radical complex were established by Marchon et al.[28] Outer-sphere, one-electron transfer from bromide, iodide, or 1,8-bis(dimethylamino)naphthalene resulted in formation of iron(III) porphyrin complexes. However, in the presence of bases with a high oxidation potential (such as pyridine), $[(TPP)Fe^{III}-O-Fe^{III}(TPP^{\bullet})]^{+}$ was formed. Imidazole ligands converted the high-spin iron(III) porphyrin cation radical to low-spin iron(III) porphyrin π-cation radical. Addition of imidazole induced also a reduction of iron(III) porphyrin cation radical to the corresponding low-spin iron(III) porphyrin complex.[29] As reported by Goff et al., a similar attempt to follow pyridine ligation by ^1H NMR spectroscopy was unsuccessful since this ligand brought immediate reduction.[29] Coordination of methoxide to the iron(III) porphyrin cation radical resulted in the conversion to the iron(IV) porphyrin.[30,31] Iron(III) tetramesitylporphyrin cation radical $[(TMP^{\bullet})Fe^{III}](ClO_4)_2$ was used as a convenient oxidizing agent to generate $[(TMP^{\bullet})Fe^{IV}O]^{+}$ from $(TMP)Fe^{IV}O$.[32]

While the reactivity of the iron(III) porphyrin radical complexes has received little study, there has been a considerable body of work done on porphyrin radical complexes of diamagnetic metal ions.[33-37] Typical reactions with a wide variety of nucleophiles, including pyridine, produced metalloporphyrins and β- or meso-substituted metalloporphyrins. The formation of meso-substituted isoporphyrins and bilitrienes was also observed for selected nucleophiles.[35] The factors which govern metalloporphyrin cation radical substitution should be also applicable to reactivity of iron porphyrin cation radicals. This raises the question whether the β-substitution or meso-substitution can occur for these iron complexes. Crossley et al. suggested a contribution of an iron tetraphenylporphyrin cation radical in generation of iron(III) β-NO_2-tetraphenylporphyrin in the reaction of $(TPP)Fe^{III}Cl$ with NO_2.[38] Reaction of $(OEP)Fe^{III}Cl$ with NO_2 produced $(meso\text{-}NO_2\text{-}OEP)Fe^{III}Cl$.[39] Two equivalents of hydroperoxide oxidize iron(III) tetrakis(4-methoxyphenyl)porphyrin to the corresponding isoporphyrin.[40] Recently, we have demonstrated that the addition of two relatively easily oxidizable nucleophiles (triphenylphosphine and nitrite anion) to iron(III) tetraphenylporphyrin cation radical $(TPP^{\bullet+})Fe^{III}(ClO_4)_2$ resulted in formation of the β-substituted derivatives, $(\beta\text{-}PPh_3^{+}\text{-}TPP)Fe^{III}Cl_2$ and $(\beta\text{-}NO_2\text{-}TPP)Fe^{III}Cl$, respectively.[41]

Considering the interesting chemistry demonstrated for metallotetraphenylporphyrin π-cation radicals of diamagnetic metal ions and pyridine and the observed nucleophile reactivity toward highly oxidized heme hemoproteins, we have embarked on the investigation of the iron(III) porphyrin π-cation radical−pyridine system in detail. In order to facilitate the detection of reaction products and to gain a better understanding of their properties in solution, we have undertaken an analysis of the paramagnetically shifted ^1H NMR and ^2H NMR spectra in selected spin/ligation states for independently synthesized spectroscopic models since the paramagnetically shifted porphyrin resonances are particularly diagnostic of changes in structure and spin, oxidation, and ligation states.[42]

Results

Characterization of High-Spin Iron(III) β-Substituted Porphyrins. Addition of pyridine to a dichloromethane solution of iron porphyrin π-cation radicals $[(TPP^{\bullet})Fe^{III}Cl][SbCl_6]$ (**1**-1) or $[(TPP^{\bullet})Fe^{III}(ClO_4)_2]$ (**1**-2) at −70 °C results in formation of several new species. The reaction is accompanied by a color change from green to red.

In order to characterize a stable reaction product, the identification of which clearly confirms the core reactivity of iron porphyrin cation radical, we focus our attention on iron(III) β-pyridiniumyltetraphenylporphyrin species (**2**), the only form

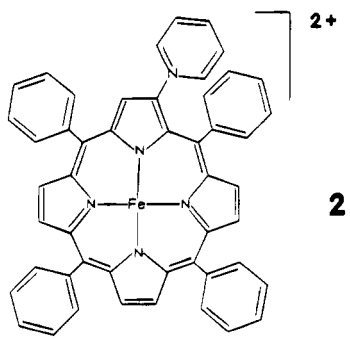

2

isolated directly from the reaction mixture. A process carried

(22) Balch, A. L.; Renner, M. *J. Am. Chem. Soc.* **1986**, *108*, 2603.
(23) Mashiko, T.; Dolphin, D.; Nakano, T.; Traylor, T. G. *J. Am. Chem. Soc.* **1985**, *107*, 3735.
(24) Mansuy, D.; Devocelle, L.; Artland, J.; Battioni, J. *Nouv. J. Chim.* **1985**, *9*, 711.
(25) (a) Collman, J. P.; Hampton, P. D.; Brauman, J. *J. Am. Chem. Soc.* **1986**, *108*, 7861. (b) Collman, J. P.; Hampton, P. D.; Brauman, J. *J. Am. Chem. Soc.* **1990**, *112*, 2977. (c) Collman, J. P.; Hampton, P. D.; Brauman, J. *J. Am. Chem. Soc.* **1990**, *112*, 2986.
(26) Traylor, T. G.; Nakano, T.; Miksztal, A. R.; Dunlap, B. E. *J. Am. Chem. Soc.* **1987**, *109*, 3625.
(27) Morehouse, K. M.; Sipe, H. J., Jr.; Mason, R. P. *Arch. Biochem. Biophys.* **1989**, *273*, 158.
(28) (a) Arena, F.; Gans, P.; Marchon, J.-C. *J. Chem. Soc., Chem. Commun.* **1984**, 196. (b) Arena, F.; Gans, P.; Marchon, J.-C. *Nouv. J. Chim.* **1985**, *9*, 505.
(29) Goff, H. M.; Phillippi, M. A. *J. Am. Chem. Soc.* **1983**, *105*, 7567.
(30) Groves, J. T.; Quinn, R.; McMurry, T. J.; Nakamura, M.; Lang, G.; Boso, B. *J. Am. Chem. Soc.* **1985**, *107*, 354.
(31) Groves, J. T.; McMurry, T. J. *Rev. Port. Quim.* **1985**, *27*, 102.
(32) Balch, A. L.; Latos-Grażyński, L.; Renner, M. W. *J. Am. Chem. Soc.* **1985**, *107*, 2983.
(33) (a) Evans, B.; Smith, K. M. *Tetrahedron Lett.* **1977**, 3079. (b) Barnett, G. H.; Evans, B.; Smith, K. M.; Besecke, S.; Fuhrhop, J.-H. *Tetrahedron Lett.* **1976**, 4009. (c) Evans, B.; Smith, K. M.; Cavaleiro, J. A. *Tetrahedron Lett.* **1976**, *4863*. (d) Evans, B.; Smith, K. M.; Cavaleiro, J. A. S. *J. Chem. Soc., Perkin Trans. 1* **1978**, 768.
(34) (a) Johnson, E. C.; Dolphin, D. *J. Tetrahedron Lett.* **1976**, 2197. (b) Gong, L.-C.; Dolphin, D. *Can. J. Chem.* **1985**, *63*, 401. (c) Dolphin, D.; Halko, D. J.; Johnson, E. C.; Rousseau, In *Porphyrin Chemistry Advances*; Longo, F. R., Ed.; Ann Arbor Science Publisher Inc.: Ann Arbor, MI, 1979; pp 119−141.
(35) (a) Padilla, A. G.; Wu, S. M.; Shine, H. J. *J. Chem. Soc., Chem. Commun.* **1976**, 236. (b) Shine, H. J.; Padilla, A. G.; Wu, S. M. *J. Org. Chem.* **1979**, *23*, 4069.
(36) (a) El Kahef, L.; ElMeray, M.; Gross, M.; Giraudeau A. *J. Chem. Soc., Chem. Commun.* **1986**, 621. (b) El Kahef, L.; Gross, M.; Giraudeau, A. *J. Chem. Soc., Chem. Commun.* **1989**, 963.
(37) Cavaleiro, J. A. S.; Neves, M. G. P. M. S.; Hewlins, M. J. E.; Jackson, A. H. *J. Chem. Soc., Perkin. Trans. 1* **1986**, 575.
(38) Catalano, M. M.; Crossley, M. J.; Harding, M. M.; King, L. G. *J. Chem. Soc., Chem. Commun.* **1984**, 1535.
(39) Fanning, J. C.; Mandel, F. S.; Gray, T. L.; Datta-Gupta, N. *Tetrahedron* **1979**, *39*, 1251.
(40) Gold, A.; Ivey, W.; Toney, G. E.; Sangaiah, R. *Inorg. Chem.* **1984**, *23*, 2932.
(41) Małek, A.; Latos-Grażyński, L.; Bartczak, T. J.; Żądło, A. *Inorg. Chem.* **1991**, *30*, 3222.
(42) La Mar, G. N.; Walker, F. A. *The Porphyrins*; Dolphin, D., Ed.; Academic Press: New York, 1979; Vol. 4, pp 61−312.

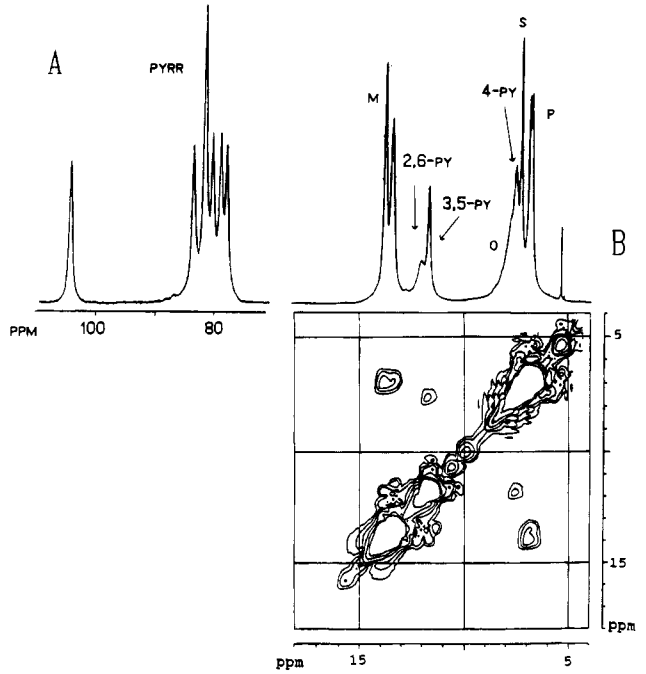

Figure 1. (Top) ^{1}H NMR spectrum of (β-py-TPP)Fe^{III}Br$_2$ in chloroform-*d* at 20 °C: (A) pyrrole resonances; (B) phenyl and pyridinium resonances. (Bottom) 300 MHz MCOSY plot for (β-py-TPP)Fe^{III}Br$_2$. Cross peaks connecting meta and para resonances of phenyl and pyridinium moieties are shown. Resonance assignment of the pyridinium ring: 2,6-py, 3,5-py, 4-py, according to the position in the ring.

out on the synthetic scale leads to isolation of a (μ-oxo)diiron(III) complex, {[(β-py-TPP)Fe^{III}]$_2$O}(ClO$_4$)$_2$, by chromatography. The infrared spectrum provides strong evidence for the presence of a bent μ-oxo-bridged diiron(III) unit. The band assigned to the asymmetric stretching vibration of the Fe^{III}–O–Fe^{III} fragment has been observed at 860 cm^{-1}.[41] In the ^{1}H NMR spectrum (data not shown) a set of pyrrole resonances in the range 15.5–13.2 ppm (25 °C, CD_2Cl_2) identifies {[(β-(py-d_5)-TPP)Fe^{III}]$_2$O}(ClO$_4$)$_2$ and reflects the asymmetry imposed by β-substitution. The position of the resonances and the observed non-Curie behavior of the isotropic shift with temperature are due to an antiferromagnetic interaction that is usual for the (μ-oxo)diiron(III) system.[41,42] The identification of the β-substituted structure has been confirmed by the independent synthesis of (β-py-TPP)Fe^{III}Br$_2$. (β-py-TPP)Fe^{III}Br$_2$ was obtained by iron insertion into β-py-TPPH$_2$ that was prepared by previously described routes.[35,36] The initially formed (μ-oxo)diiron(III) complex was split with suitable acids to obtain (β-py-TPP)Fe^{III}Cl$_2$ (**2**-Cl$_2$), (β-py-TPP)Fe^{III}Br$_2$ (**2**-Br$_2$), (β-py-TPP)Fe^{III}I$_2$ (**2**-I$_2$), and (β-py-TPP)Fe^{III}(ClO$_4$)$_2$ (**2**-(ClO$_4$)$_2$). The EPR spectrum of (β-py-TPP)Fe^{III}Br$_2$ (not shown, measured in frozen dichloromethane, −194 °C) is typical for the high-spin iron(III) porphyrin pattern ($g_\perp = 6$, $g_\parallel = 2$).[41]

The ^{1}H NMR data have been analyzed in the context of the symmetry resulting from the β-substitution (Figures 1–3; Table 1) in multiple spin/ligation states. Porphyrins of structure **2** have seven distinct pyrrole positions and four different meso positions. For a five-coordinate species, eight ortho, eight meta, and four para protons will be distinguishable because of the essentially perpendicular relation between the meso phenyl plane and the plane of adjacent pyrrole rings as well as the restricted rotation about the meso-carbon-to-phenyl bond. Two ortho and two meta β-pyridine resonances are expected for the same reasons. In the case of rapid rotation of the phenyl rings or in the case of two identical axial ligands, the number of ortho and meta resonances is reduced by a factor of 2.[41,42] The number of resonances can be considered as a diagnostic feature of the

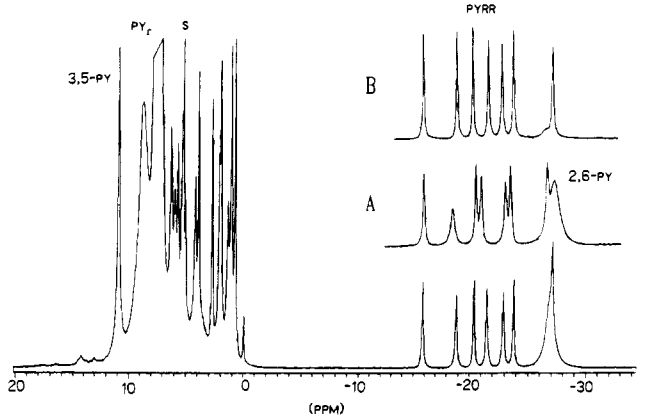

Figure 2. 300 MHz ^{1}H NMR spectra of (β-py-TPP)Fe^{III}Cl$_2$ after addition of 6 equiv of pyridine in dichloromethane-d_2 at −70 °C. Insets A and B show the proton resonances of the 2,6-pyridine and pyrrole protons: (A) 1 equiv of pyridine; (B) 6 equiv of pyridine and 44 equiv of pyridine-d_5 added under the same conditions as for (A).

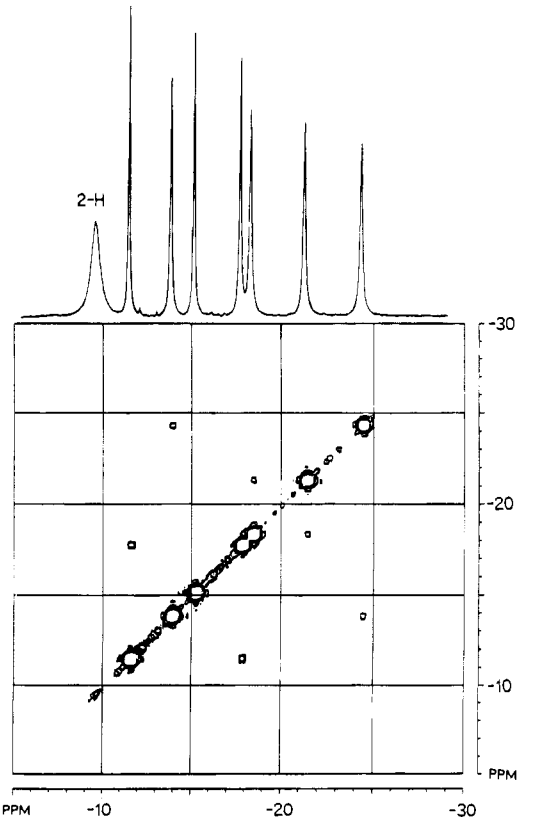

Figure 3. (Top) Portion of the 300 MHz ^{1}H spectrum of [(β-py-TPP)Fe^{III}(1-MeIm)$_2$]Br$_2$ in chloroform-*d* at 20 °C. (Bottom) 300 MHz MCOSY plot for [(β-py-TPP)Fe^{III}(1-MeIm)$_2$]Br$_2$. Cross peaks connecting resonances of protons located on the same pyrrole ring are shown. Resonance assignment: 2-H, 2-H proton of 1-MeIm; unlabeled resonances correspond to pyrrole protons. Cross peaks connecting pyrrole resonances of unsubstituted pyrrole rings are shown.

number of ligands at the available axial positions and/or internal rotation in the [(β-py-TPP)Fe^{III}]$^{2+}$ moiety. The ^{1}H NMR spectrum of the high-spin (β-py-TPP)Fe^{III}Br$_2$ (**2**-Br$_2$) complex is shown in Figure 1. Resonance assignments have been made on the basis of relative intensities, line widths, and site specific deuteration. The direct comparison to iron(III) tetraphenylporphyrin complexes and to the previously characterized β-substituted complexes [(β-PPh$_3$-TPP)Fe^{III}]$^{2+}$ and [(β-NO$_2$-TPP)Fe^{III}]$^+$ facilitated the assignment.

Six downfield pyrrole resonances have been identified for the high-spin complex **2**-Br$_2$ (Figure 1). Five of them, including one with an intensity of two protons, are spread near the position

Table 1. ^{1}H Chemical Shifts for (β-Pyridiniumyltetraphenylporphyrinato)iron(III) Complexes[a]

	Pyrrole Resonances						
2-Cl_2	103.7	82.7	80.5	80.5	80.5	78.2	77.4
2-Br_2	105.2	84.7	82.8	82.8	81.4	80.0	79.0
2-I	98.5	76.8	74.2	73.9	72.7	72.1	69.4
2-$(ClO_4)_2$	55.6	36.5	32.2	24.9	23.7	20.6	20.6

	meso-phenyl resonances			β-pyridinium resonances		
	ortho	meta	para	2,6-H	3,5-H	4-H
2-Cl		12.9 12.6	6.4	10.8	10.9	9.2
2-Br	7.6	13.9 13.5	7.41	12.0	11.9	7.4
2-I	10.1 9.8	14.4 14.1	9.7 8.5 7.8	13.7	12.4	8.0

[a] Solvent is chloroform-*d*; all measurements at 20 °C.

typical for high-spin iron(III) tetraphenylporphyrins (≃80 ppm).[41,42] The most unusual resonance occurs ca. 20 ppm downfield with respect to the center of the remaining six. It seems logical to assign this one with the largest downfield shift to the unique, β-substituted pyrrole. The β-substitution influences the σ-delocalization mechanism for the spin density at the substituted pyrrole and also has a noticeable impact on the remaining three pyrrole rings. The line width of the most downfield shifted pyrrole resonance increases in the order $I^- < Br^- < Cl^-$ (135, 205, and 450 Hz, respectively, at 20 °C). The trend parallels are seen in high-spin, iron(III) tetraphenylporphyrins. The anion dependence of line width is a result of zero field splitting of the ground electronic state that is dependent on the axial ligand.[43] The temperature dependencies (T^{-1}) of pyrrole paramagnetic shifts demonstrated some curvature; this curvature is related to the ZFS generated dipolar contribution. The data for the bromide or iodide forms, where the resolution is optimal, were examined in detail. In the case of (β-py-TPP)$Fe^{III}I_2$ seven pyrrole resonances have been clearly resolved (Table 1). Figure 1 shows an expansion of the 18-4 ppm region of the (β-py-TPP)$Fe^{III}Br_2$ spectrum. Three pyridinium resonances are readily assigned on the basis of the direct comparison of (β-py-TPP)$Fe^{III}Br_2$ and (β-(py-d_5)-TPP)$Fe^{III}Br_2$ spectra. The para resonance (4-py) is distinguished on the basis of its intensity. The greater line width of the ortho proton (2,6-py) is consistent with the fact that these protons are closest to the iron and the most affected by dipolar contribution. This assignment has been confirmed by a two-dimensional magnitude COSY experiment. The cross-peaks for the narrower resonances of the pyridinium or phenyl protons are clearly apparent. Two resonances at 13.9 and 13.4 ppm (20 °C) are assigned to the meta meso-phenyl protons (M) of (β-py-TPP)$Fe^{III}Br_2$. The pattern of meta resonances and pyridinium resonances can be explained by coordination of two bromide ligands at the axial positions. Such geometry has been determined for (β-PPh_3−TPP)$Fe^{III}Cl_2$ in the solid state and for Cl^-, Br^-, and I^- in solution.[41] In this regard the (β-py-TPP)$Fe^{III}Br_2$ complex resembles other iron porphyrin complexes that have peripheral substituents which bear positive charge[41,44] and iron complexes of octaethyloxoporphyrin, where the positive charge is situated on the ligand outer atoms.[45] Such a "zwitterionic" structure

(43) (a) La Mar, G. N.; Eaton, G. R.; Holm, R. H.; Walker, F. A. *J. Am. Chem. Soc.* **1973**, *95*, 63. (b) Behere, D. V.; Birdy, R.; Mitra, S. *Inorg. Chem.* **1982**, *21*, 386. (c) Balch, A. L.; La Mar, G. N.; Latos-Grażyński, L.; Renner, M. *Inorg. Chem.* **1985**, *21*, 2432.

(44) (a) Ivanca, M. A.; Lappin, A. G.; Scheidt, W. R. *Inorg. Chem.* **1991**, *30*, 711. (b) Rodgers, K. R.; Reed, R. A.; Su, Y. O.; Spiro, T. G. *Inorg. Chem.* **1992**, *31*, 2688.

(45) Balch, A. L.; Latos-Grażyński, L.; Noll, B. C.; Olmstead, M. M.; Szterenberg, L.; Safari, N. *J. Am. Chem. Soc.* **1993**, *113*, 1422.

Table 2. ^{1}H Chemical Shifts of Pyrrole Resonances for Low-Spin (β-Pyridiniumyltetraphenylporphyrinato)iron(III) Complexes[a]

[**2**-$(py)_2$]Cl_2[b]	−8.31	−8.89	−9.43	−11.13	−11.50	−11.67	−13.26
[**2**-$(py)_2$]Br_2[b]	−8.56	−9.00	−9.38	−10.78	−11.49	−11.80	−12.92
[**2**-$(py)_2$]$(ClO_4)_2$[b]	−8.07	−8.12	−9.40	−10.49	−10.76	−11.64	−12.60
[**2**-(1-MeIm)$_2$]Cl_2[c]	−10.85	−13.66	−15.29	−17.60	−17.74	−21.59	−24.25
[**2**-(1-MeIm)$_2$]Br_2[c]	−11.94	−13.93	−14.96	−17.65	−18.46	−20.99	−23.96

[a] All measurements at 20 °C. [b] 100 equiv of pyridine-d_5 added. [c] 6 equiv of 1-MeIm added.

increases the local concentration and the likelihood of second anionic ligand coordination without its large excess so the solution properties are determined by bis-ligated species.

Spectral Characterization of Low-Spin Iron(III) β-Substituted Porphyrins. Addition of pyridine to **2**-Br_2 at 20 °C converts high-spin iron porphyrins into their low-spin counterparts [**2**-$(py)_2$]$_2$ (Figure 2). For analytical purposes, the characteristic set of seven, upfield-shifted pyrrole resonances between −15 and −30 ppm in the ^{1}H NMR spectrum is of importance to the characterization of the low-spin products. High-spin **2**-Cl_2 and **2**-Br_2 are relatively resistant to nitrogen ligand coordination. In an equimolar mixture of **2**-Br_2 and (TPP)Fe^{III}Br, the addition of two pyridine equivalents selectively produces [(TPP)$Fe^{III}(py)_2$]. Such a conversion for the β-substituted form is not achieved up to a 1:80 **2**-Br_2 to pyridine molar ratio. To establish the stoichiometry of the reaction we carried out the titration of **2**-Cl_2, **2**-Br_2, and **2**-$(ClO_4)_2$ with pyridine and 1-MeIm (Table 2). In the case of the more strongly coordinating 1-MeIm, the six-coordinate species was formed at 20 °C with only 6 equiv of 1-MeIm. We assigned the two bound 1-MeIm ligands by integration of resonances assigned to the pyrrole and the 2-H of 1-MeIm protons.

In the cases of the pyridine adducts, we observed a smooth upfield change of chemical shifts as the pyridine concentration was increased for low-spin and high-spin species at 20 °C (data not shown). This effect was explained by the exchange between forms which coordinate different numbers of pyridine ligands. The ligand resonances were not observed. In an experiment carried out at −70 °C (under conditions of slower exchange) we found, via integration of the 3,5-H of coordinated pyridine and pyrrole resonances, that two pyridine molecules are coordinated in the low-spin form. Selective broadening of the pyrrole resonance at −18 ppm at lower concentrations of pyridine has been observed (Figure 2). A similar influence of 1-MeIm concentration on pyrrole line width at 20 °C has been also found (data not shown), but in this system the resonance at −15 ppm demonstrated the effect. We have observed a dependence of the pyrrole spectrum pattern on the counteranion (Table 2). As the coordination sphere of iron(III) is saturated with pyridine, the spectral differences can be accounted for by formation of tight ion pairs $\{[(\beta\text{-py-TPP})Fe^{III}(py)_2]X\}^+$ due to the two uncompensated charges of $[(\beta\text{-py-TPP})Fe^{III}]^{2+}$.

The temperature dependencies of the pyrrole chemical shifts for the low-spin complexes vary lineary with T^{-1} (data not shown), but the extrapolated lines do not pass through the positions expected for the the diamagnetic references; this has been observed for other low-spin β-substituted iron(III) tetraphenylporphyrins.[41]

The two-dimensional COSY experiment is especially effective in the determination of the pairs of resonances that belong to the same pyrrole ring (Figure 3). Cross peaks that connect spin-coupled protons located on the same pyrrole ring are readily apparent in a COSY map obtained for [(β-py-TPP)Fe^{III}(1-MeIm)$_2$]Br_2. The unique uncoupled resonance from the β-substituted ring (−15 ppm) also exhibits the largest dynamic broadening in the course of titration (data not shown). It seems that the exchange broadening in the **1**-Cl_2−pyridine or **1**-Cl_2−

1-MeIm systems is the most pronounced for the resonances where the shift differences between high-spin and low-spin forms are the largest.

The addition of pyridine or 1-MeIm to (β-py-TPP)$Fe^{III}X_2$ (X = halogenide anion) occurs in following steps:

$$(\beta\text{-py-TPP})Fe^{III}X_2 + py \overset{K_1}{\rightleftharpoons} [\beta\text{-py-TPP})Fe^{III}(X)(py)]X \quad (1)$$

$$[(\beta\text{-py-TPP})Fe^{III}(X)(py)]X + py \overset{K_2}{\rightleftharpoons} [(\beta\text{-py-TPP})Fe^{III}(py)_2]X_2 \quad (2)$$

$$[(\beta\text{-py-TPP})Fe^{III}(py)_2]X_2 \overset{K_3}{\rightleftharpoons} \{[(\beta\text{-py-TPP})Fe^{III}(py)_2]X\}^+ + X^- \quad (3)$$

Analogous reactions have been seen for (TPP)$Fe^{III}X$ where usually $K_1 < K_2$.[46-48] However, in the case of pyridine the mixed ligand complexes [(TPP)$Fe^{III}X(py)$] were obtained in the tetraphenylporphyrin series.[47] The additional positive charge of the pyridinium substituents seems to add additional stabilization against halide ligand dissociation for both the starting material and the [(β-py-TPP)$Fe^{III}(X)(py)$]X species.

Reaction of Iron(III) Tetraphenylporphyrin Cation Radical [(TPP$^{\bullet}$)Fe^{III}Cl][$SbCl_6$] with Pyridine. Addition of pyridine-d_5 to a dichloromethane solution of **1**-1 or **1**-1-d_8 at −70 °C produces a set of new paramagnetic species. The formation of new species is readily detected by the changes observed in the ^1H NMR (Figure 4) and ^2H NMR (Figure 5) spectra. Preliminary analysis of the spectra leads to conclusion that the pattern of specifically identified pyrrole resonances is consistent with a drastic symmetry lowering of the reaction products as compared to the highly symmetrical starting materials.

Three types of ring-substituted products could be easily distinguished. The symmetry lowering led to spectra which contain respectively seven, four, and two pyrrole resonances which are assigned to iron complexes of β-R-tetraphenylporphyrin (**2**), 5-R-isotetraphenylporphyin (**3**), and 5,10-di-R-tetraphenylporphodimethene (**4**), where R = pyridiniumyl (*vide infra*). In particular the pattern with two resonances does not have any precedent in the spectroscopy of paramagnetic iron tetraphenylporphyrin complexes and their derivatives.

The resonances of **1**-1 are severely broadened after addition of 1 equiv of pyridine (Figure 4, trace B). This suggests that the cation-radical forms a pyridine adduct, which remains in fast exchange with **1**-1. At this stage we have also detected a characteristic pattern of pyrrole resonances located at the 150−100 ppm range (−70 °C). They have been unequivocally assigned to high-spin iron(III) porphyrin derivatives **3**-1 and **4**-1. The formation of **3**-1 and **4**-1 is accompanied by the production of low-spin ($S = {}^1/_2$) [(TPP)$Fe^{III}(py)_2]^+$ (**5**-py_2) in a concentration comparable to high-spin species. Detailed analysis of the spectra reveals that other species are formed in a small concentration in the process. One, **2**-1 (Figure 4, trace C and inset) is typical for a low-spin state with an upfield-shifted pyrrole pattern. In addition a rather complex multiplet centered around −50 ppm is seen (Figure 4, trace C and inset). We have noticed that this set of resonances can be accounted for

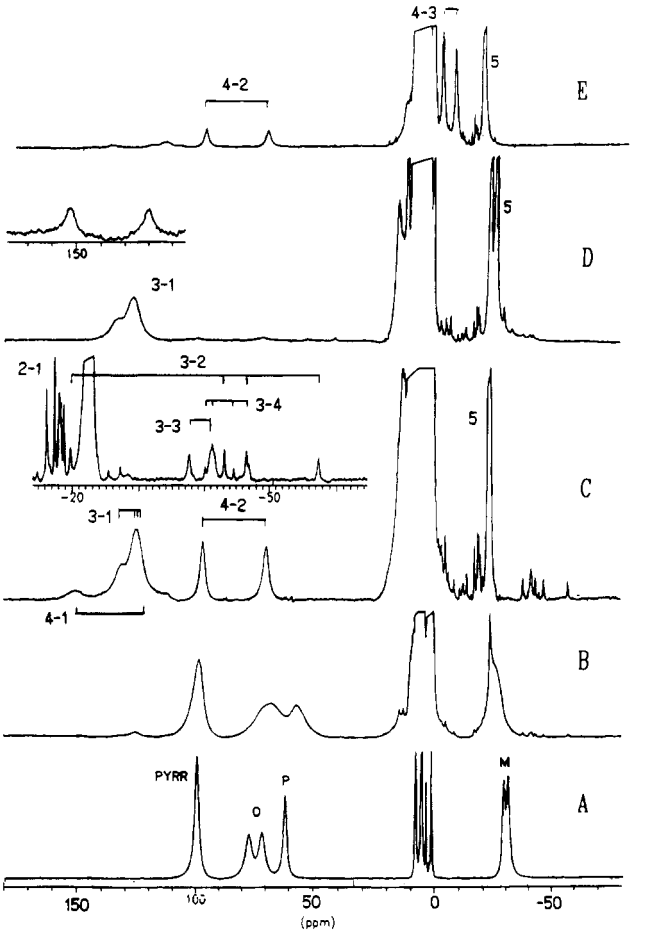

Figure 4. Trace A: ^1H NMR spectrum of [(TPP$^{\bullet}$)Fe^{III}Cl][$SbCl_6$] (**1**-1) in dichloromethane-d_2 at −70 °C. Trace B: ^1H NMR spectrum from the same solution after addition of 1 equiv of pyridine-d_5 at −70 °C. Trace C: ^1H NMR spectrum from the same solution as in (B) after addition of 2 equiv of pyridine-d_5 at −70 °C. The inset presents the details of the upfield part of the spectrum. Trace D: ^1H NMR spectrum of [(TPP$^{\bullet}$)Fe^{III}Cl][$SbCl_6$] (**1**-1) in dichloromethane-d_2 at −70 °C after addition of 5 equiv of pyridine-d_5, followed by addition of HCl in dichloromethane-d_2. The inset presents the result of the subtraction of the spectra obtained before and after the HCl addition. Trace E: ^1H NMR spectrum of [(TPP$^{\bullet}$)Fe^{III}Cl][$SbCl_6$] (**1**-1) in dichloromethane-d_2 at −70 °C after addition of 50 equiv of pyridine-d_5 in one portion. The pyrrole resonances due to unstable species are labeled according to the abbreviation used in the text. Resonance assignments: pyrr, pyrrole protons of **1**-1; phenyl ring, o, the ortho proton, m, the meta proton, and p, the para proton.

by three species: **3**−2, **3**−3, and **3**−4. These are labeled directly on trace C of Figure 4. The resonances were correlated in four-peak sets, based on similarities in line width and intensities. These forms are extremely unstable and disappear after addition of larger amount of pyridine at −70 °C or when the sample was warmed to −40 °C. At the present stage of investigation we can only suggest that the position of resonances reflects a presence of iron(III) coordinated equatorially by isoporphyrin in the intermediate spin state $S = {}^3/_2$ or as iron(IV) ($S = 1$). These forms exist only in the presence of excess of the strong oxidizing agent i.e., **1**-Cl. We have observed substantial changes after addition of the second equivalent of pyridine. The resonances of the cation radical have been completely replaced with those of a new intermediate **4**-2 which can be confidently identified as a porphodimethene derivative with characteristic pyrrole resonances located at 68.5 ppm (840 Hz) and 96.0 ppm (785 Hz) (line widths at −70 °C) (Figure 4, trace C). The identity of the two pyrrole resonances has been confirmed by ^2H NMR spectral studies where the process has been followed on a sample that was specifically deuterated at

(46) La Mar, G. N.; Bold, T. J.; Satterlee, J. D. *Biochim. Biophys. Acta* **1977**, *489*, 189.
(47) Scheidt, W. R.; Lee, Y. J.; Geiger, D. K.; Taylor, K.; Hatano, K. *J. Am. Chem. Soc.* **1982**, *104*, 3367.
(48) (a) Adams, K. M.; Rasmussen, P. G.; Scheidt, R. W.; Hatano, K. *Inorg. Chem.* **1979**, *18*, 1892. (b) Ogoshi, H.; Sugimoto, H.; Watanabe, E.; Yoshida, Z.; Maeda, Y.; Sakai, H. *Bull. Chem. Soc. Jpn.* **1981**, *54*, 3414. (c) Gunter, M. J.; McLaughlin, G. M.; Berry, K.; Murray, K. S.; Irving, M.; Clark, P. E. *Inorg. Chem.* **1984**, *23*, 283.

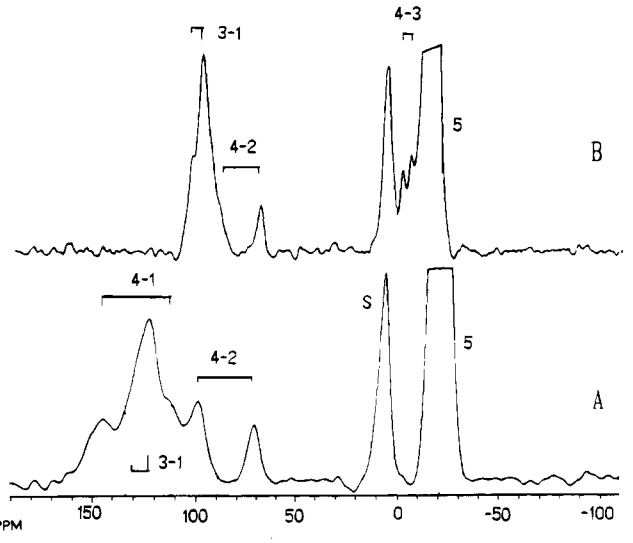

Figure 5. ^{2}H NMR spectra of [(TPP•-d_8)Fe^{III}Cl][SbCl$_6$] (**1**-1) at dichloromethane with 50-fold excess of pyridine: (A) at −70 °C; (B) at −40 °C. Resonance assignments follow those of Figure 5; S = solvent.

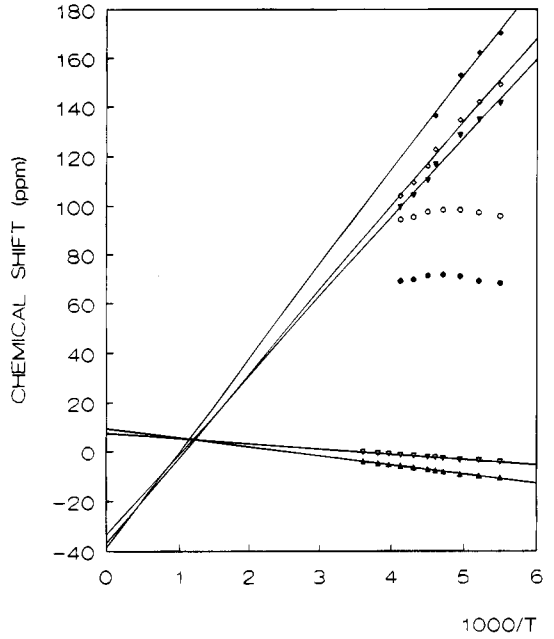

Figure 6. Plots of the chemical shifts of pyrrole resonances versus 1/T (in dichloromethane-d_2): **3**-1, ◇, ▼; **4**-1, ◆; **4**-2, ○, ●; **4**-3, ▽, ▲.

the pyrrole β position. The data are shown in Figure 5. The species **4**-2 is stable at −70 °C. Further gradual addition of pyridine up to 50 equiv at this temperature does not change the composition of solution.

Addition of Cl_2 dissolved in CD_2Cl_2 increased the concentration of **3**-2 considerably (data not shown). The forms **4**-1 and **4**-2 decomposed after the addition of HCl in CD_2Cl_2 to the sample at −70 °C. The high-spin iron(III) isoporphyrin derivative **3**-1 remained under this conditions (Figure 4, trace D). The inset in trace D reveals that the formation of two species (*i.e.*, **3**-1 and **4**-1) is necessary to account for the complex set of resonances in trace C of Figure 4 at the 150-100 ppm region.

A substantial difference in reactivity of **1**-1 was observed when 50 equiv of pyridine was added in one portion to **1**-1 at −70 °C (precaution was taken to cool down the pyridine solution to −70 °C before addition to the reaction mixture). Under these experimental conditions a new form, **4**-3, with two upfield-shifted pyrrole resonances at −3.44 ppm (365 Hz) and −9.25 ppm (395 Hz) (line widths at −70 °C) was observed (trace E, Figure 4). The spectra assignment was confirmed by the ^{2}H NMR spectrum (Figure 5, trace B). On warming of the sample from −70 to −40 °C, we observed a transformation of **4**-1 and **4**-2 to **4**-3 in the presence of 50 equiv of pyridine. Further warming to 25 °C resulted in a irreversible decomposition of **3** and **4**. Low-spin and high-spin derivatives of **2** remained as the major, stable reaction products at 25 °C. Curie plots for the pyrrole resonances of the newly detected intermediates are collected in Figure 6. The experimental data for **4**-3 show linear behavior over the accessible temperature range. The extrapolated intercepts are located at 7.38 and 9.35 ppm, which are only slightly downfield of the anticipated diamagnetic positions. The pyrrole shifts measured for macrocycles with the structures similar to **3** and **4** (5,15-dihydroxyporphodimethenes, 6.69 and 6.48 ppm)[34c] and diamagnetic metalloisoporphyrins[49] have been used as the diamagnetic standard. The pyrrole resonances of **4**-2 show anomalous behavior. Both plots show some curvature over the accessible temperature range; anti-Curie slopes are observed for the lowest temperature range. An attempt of a linear extrapolation with respect to T^{-1} resulted in unrealistic diamagnetic intercepts of 77.1 and 66.5 ppm for **4**-2 and −30 to 40 ppm for **3**-1 and **4**-1. These deviations cannot be accounted for by the chemical exchange since the measured paramagnetic shifts are not dependent on a pyridine concentration but should be related to the specific electronic states.

Reaction of Iron(III) Tetraphenylporphyrin Cation Radical [(TPP•)Fe^{III}(ClO$_4$)$_2$] (1-2) with Pyridine. The titrations of **1**-2 and **1**-2-d_8 with pyridine-d_5 were followed by ^{1}H NMR and ^{2}H NMR in two parallel experiments. The results are presented in Figures 7 and 8, respectively. The characteristic shifts of the pyrrole resonances are collected in Table 3. The ^{2}H NMR experiments, carried out for pyrrole-deuterated iron(III) porphyrin π-cation radical (**1**-2-d_8) (Figure 8), unequivocally confirmed the pyrrole resonance assignments in Figure 7. The cation radical **1**-2 undergoes aquation in dichloromethane by residual water to give [**1**-(H$_2$O)$_2$](ClO$_4$)$_2$ that complicates the ligation equilibria in the system.[28] [**1**-(OH)(H$_2$O)](ClO$_4$) and **5**-(OH) were postulated as necessary intermediates in the formation of [(TPP)Fe−O−Fe(TPP•)]$^+$.[28] The ^{1}H NMR spectra of **1**-2 and related (TMP•)Fe^{III}(ClO$_4$)$_2$ were found to be very sensitive to solvent and temperature.[31] Reed *et al.* have previously demonstrated that (TPP)Fe^{III}(ClO$_4$) becomes [(TPP)-Fe(H$_2$O)$_2$]ClO$_4$ upon addition of aqueous perchloric acid.[50] Previous studies demonstrated that the aquation processes are essential in the generation of highly oxidized species via proton acid−base equilibria of coordinated water and plausible disproportionation pathways.[31,44,51]

In our experiments an addition of pyridine to **1**-2 (−70 °C) in substoichiometric amounts shifts the acid−base equilibria because this base acts primarily as a proton scavenger. However a 1:2 molar ratio is sufficient to convert all of cation radical into its pyridine derivatives (Figure 7, trace A; Figure 8, trace A). The pyrrole resonance position and line width of **1**-3 depend on the pyridine concentration (e.g., 9.95 ppm at −70 °C, 1:50 molar ratio). This suggests that fast exchange occurs between

(49) (a) Lee, W. A.; Bruice, T. C. *Inorg. Chem.* **1986**, *25*, 131. (b) Schmidt, E. S.; Bruice, T. C.; Brown, R. S.; Wilkins, C. L. *Inorg. Chem.* **1986**, *25*, 4799.

(50) Kastner, M. E.; Scheidt, W. R.; Mashiko, T.; Reed, C. A. *J. Am. Chem. Soc.* **1978**, *100*, 667.

(51) (a) Calderwood, T. S.; Lee, W. A.; Bruice, T. C. *J. Am. Chem. Soc.* **1985**, *107*, 8272. (b) Lee, W. A.; Calderwood, T. S.; Bruice, T. C. *Proc. Natl. Acad. Sci. U.S.A.* **1985**, *82*, 4301. (c) Groves, J. T.; Gilbert, J. A. *Inorg. Chem.* **1986**, *25*, 125. (d) Calderwood, T. S.; Bruice, T. C. *Inorg. Chem.* **1986**, *25*, 3722. (e) Swistak, C.; Mu, X. H.; Kadish, K. M. *Inorg. Chem.* **1987**, *26*, 4360.

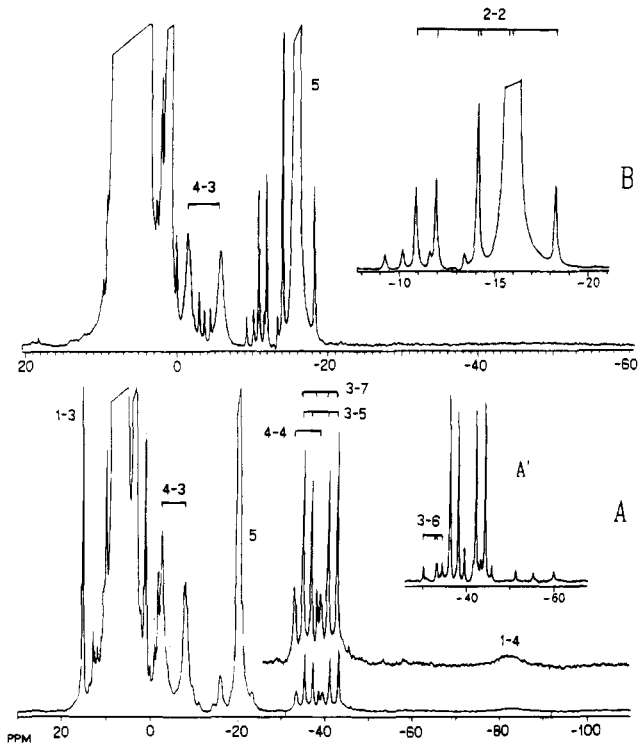

Figure 7. Trace A: ^{1}H NMR spectrum of (TPP$^{\bullet}$)Fe^{III}(ClO$_4$)$_2$ (**1**-2) in dichloromethane-d_2 at −60 °C after addition of 50 equiv of pyridine-d_5. Inset A′ presents the system under similar conditions but with a sample prepared without purification of dichloromethane-d_2. Trace B: ^{1}H NMR spectrum from the same solution at −30 °C. Derivatives in the **3**-n and **4**-n classes are of 5-R-isotetraphenylporphyrins and 5,15-di-R-tetraphenylporphodimethenes, respectively.

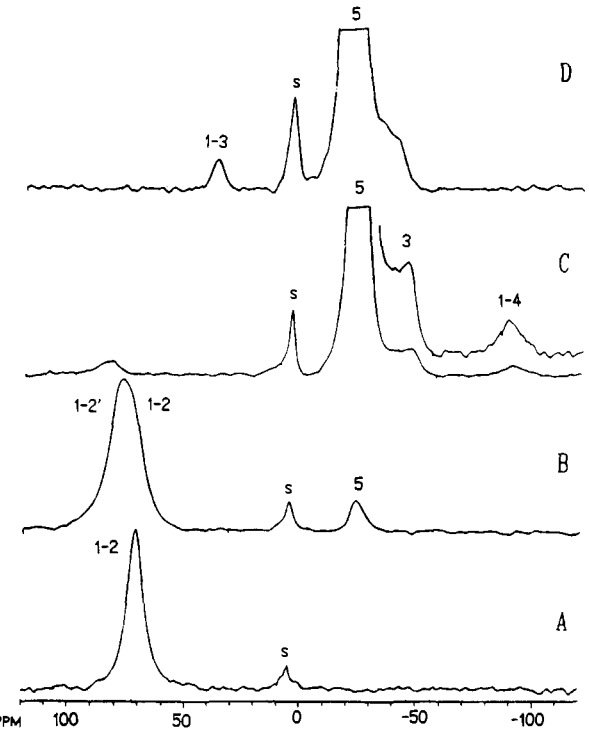

Figure 8. Trace A: ^{2}H NMR spectra of [(TPP$^{\bullet}$-d_8)Fe^{III}(ClO$_4$)$_2$ (**1**-2) in dichloromethane at −70 °C. Trace B: ^{2}H NMR spectrum from the same solution after addition of 2 equiv of pyridine at −70 °C. Trace C: ^{2}H NMR spectrum from the same solution after addition of 5 equiv of pyridine at −70 °C. Trace D: ^{2}NMR spectra of [(TPP$^{\bullet}$-d_8)-Fe^{III}(ClO$_4$)$_2$ (**1**-2) after addition of 10 equiv of pyridine at −70 °C and warming to −50 °C. Resonance assignments follow those of Figure 5; S = solvent.

forms which contain different numbers of coordinated pyridine ligands. The formation of **1**-3 is accompanied by generation of **5**. The simultaneous observation of pyrrole resonances of pyridine adducts of **1**-3 and **5** suggests that the rate of electron exchange between these two species is slow on the ^{1}H NMR time scale. Under identical conditions the complete conversion of the independently synthesized (TPP)Fe^{III}(ClO$_4$) and its hydrated forms to low-spin products [(TPP)Fe^{III}(py)$_2$]$^+$ has been achieved even for the 1:2 molar ratio (data not shown). The general reactivity pattern, i.e., an attack on the porphyrin macrocycle, remained the same for **1**-2 as for **1**-1. In particular, the formation of an iron isoporphyrin intermediate is well documented. The four pyrrole resonances of **3**-5 are readily detected after addition of pyridine-d_5 (Figure 7, trace A; Figure 8, traces C and D). The species are unstable and disappear when additional pyridine is added.

A variety of isoporphyrin derivatives could be generated depending on the solvent purification as illustrated in Figure 7 (inset A′). A pyrrole resonance with unusually high paramagnetic shift (−91 ppm, −70 °C) has been tentatively assigned to iron(IV) tetraphenylporphyrin **1**-4. Gradual growth of pyrrole resonances at the 0 to −20 ppm range, assigned to **4**-3 and to the low-spin form of **2**-2 (Figure 7, trace B) have been also seen. Under the conditions used in this work, some of the intermediates are extremely unstable. The intermediates **3**-n and **4**-n disappear within the temperature range −80 °C to −30 °C. This process is thermally irreversible. However, the relatively stable **4**-3 species has been observed at small concentrations even at 10 °C for the period of time sufficient to collect the ^{1}H NMR spectrum. It can be generated from two substrates **1**-1 and **1**-2 and results from conversion of **4**-2 in the presence of excess pyridine. This leads to the suggestion that the pyridine, rather than an ionic ligand, is coordinated to iron(III) in **4**-3. A Curie plot of the temperature dependence

Table 3. ^{1}H Chemical Shifts of Pyrrole Resonances of Selected Species Formed in Iron(III) Tetraphenylporphyrin Cation Radical−Pyridine Systems[a]

1−3	9			
1−4	−90.4			
3−1	134.5	128.4		
3−5	−37.92	−41.52	−44.3	−46.4
4−1	152.8	116.5		
4−2	96.0	68.5		
4−3	−3.4	−9.25		

[a] In dichloromethane-d_2; all measurements at −70 °C.

of the chemical shift of the pyrrole resonance of **1**-3 is shown in Figure 9. The resonance shows linear anti-Curie behavior. The negative slope of the Curie plot may result from the fact that the species in the low-spin state remains in fast ligand exchange with its corresponding high-spin adduct. Thermal high-spin−low-spin equilibria, possibly accompanied by changes of the a_{1u}−a_{2u} porphyrin radical ground states, may account for the temperature dependence of the chemical shift.[29,52] Upon warming, **1**-3 is unstable and disappears completely at −40 °C. Curie plots for the upfield shifted pyrrole resonances of **3**-5 and **1**-4 (Figure 9) are consistent with linear behavior over the limited temperature range. However, the extrapolated intercepts at infinite temperature deviate considerably from the anticipated diamagnetic positions.[34c,35,49]

Replacement of the pyridine by a sterically hindered derivative, i.e. 2,4,6-collidine (1:10 molar ratio, −70 °C) directed the reaction of **1**-2 into the formation of known[28] [(TPP$^{\bullet}$)Fe^{III}−O−Fe^{III}(TPP)]$^+$ as confirmed by ^{1}H NMR. This species is also formed when pyridine is added to an equimolar mixture of

(52) (a) Morishima, I.; Shiro, Y.; Nakajima, K. *Biochemistry* **1986**, *25*, 3576. (b) Rachlewicz, K.; Latos-Grażyński, L. *Inorg. Chim. Acta* **1988**, *144*, 213.

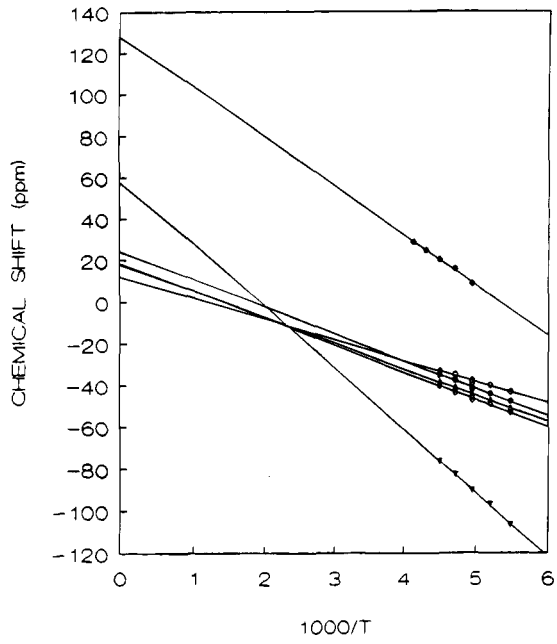

Figure 9. Plots of the chemical shifts of pyrrole resonances versus $1/T$ (in dichloromethane-d_2): **1**-3, ●; **1**-4, ▼; **3**-5, ○, ●, △, ◇.

5-ClO_4 and **1**-$(ClO_4)_2$ in dichloromethane at 20 °C (results not shown). The experiment with collidine demonstrates that pyridine acts as a nucleophile which attacks the porphyrin core at the meso or β-positions. One could expect that the pyridine acts only as a proton scavenger,[28] but this definitely is not the case.

Discussion

Reaction of Iron(III) Tetraphenylporphyrin Cation Radical with Pyridine. Structural Consideration. The reactions between iron porphyrin π-cation radicals and pyridine as a nucleophile are complex and definitely require reconsideration. This prompted us to analyze the macrocycle structures of the anticipated products in order to get necessary a structure–spectral pattern correlation. By analogy to previous studies of cation radicals and metalloporphyrin π-dications derived from diamagnetic metalloporphyrins, with the large variety of nucleophiles including pyridine (CH_3O^-, OH^-, NO_2^-, SCN^-, PPh_3),[30,33-43] the following tetraphenyltetrapyrrole macrocycles are expected to be formed: β-R-tetraphenylporphyrin (**2**),[34-37,41] 5-R-isotetraphenylporphyrin (**3**),[30,33c,33d,34,35,37,40,49,53-56] and 5,10-di-R-tetraphenylporphodimethene (**4**).[33c,33d,34,57-61] The *anticipated* structures of the *meso*-substituted forms are presented as follows:

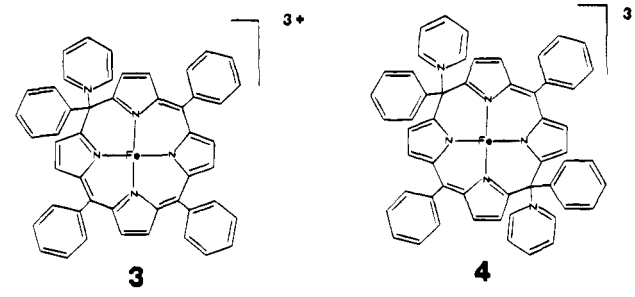

3 **4**

An alternative structure to 5,10-di-R-tetraphenylporphodimethene (**4**) involves simultaneous meso- and β-substitution.[37] Only β-substituted pyridine analogs were identified in the reaction of zinc(II) tetraphenylporphyrin π-cation radical and pyridine.[34-37] The zinc(II) isoporphyrin intermediate was suggested by Dolphin et al. for this reaction.[34c] β-Pyridine substitution markedly lowers the symmetry of the iron porphyrin from the effective D_{4h} (C_{4v}) of parent iron porphyrin π-cation radical. This is reflected in the ^1H and ^2H NMR spectra by a unique pattern of seven pyrrole resonances. The ^1H NMR data of iron isoporphyrins have been analyzed on the presumption of effective C_s symmetry.[40] In this case, there are four distinct pyrrole positions and three meso positions. Two stereoisomers can be expected as the consequence of the C5 saturation as phenyl rings can be located in *axial* or *equatorial* positions. Porphodimethene macrocycles are nonplanar with folding with respect to the 5,15-axis as a consequence of saturation at C5,15 positions.[60,61] Three stereoisomers are possible on the basis of 5,15-phenyl rings orientation, i.e., syn–axial (*aa*, C_{2v}), anti–axial–equatorial (*ae*, C_s), and syn–equatorial (*ee*, C_{2v}) analogously to the pattern precisely established for 5,15-dialkyl-5,15-dihydro-2,3,7,8,12,13,17,18-octaethylporphyrins and its complexes[60] and 5,15-diallyltetraphenylporphodimethene.[61] In addition, a quasi-planar structure (*dd*) can be considered with two possible isomers differentiated by the location of the pyridine with the two pyridine rings on the same (C_{2v}) or different (C_{2h}) sides of the porphyrin plane. Two pyrrole resonances are expected for the C_{2v} and C_{2h} geometries and four in the case of the C_s geometry. Steric hindrance, which usually plays the determining role in geometric structures, seems to be very similar for all roofed isomers since the phenyl and pyridine substituents are of similar size. For the sake of simplicity, our considerations have not included effects related to axial ligand coordination. The formation of a β-substituted porphyrin does not require any drastic changes in the macrocycle configuration, although tight packing is expected for β-pyridine and neighboring *meso*-phenyl rings. On the other hand, saturation at the 5- and 15-positions would result in a characteristic porphodimethene structure with severely restricted access to the metal from the one side of the macrocycle.[60e] The identical pyrrole resonance multiplicity should be demonstrated for each oxidation/ligation/spin state for any considered structure. On the basis of these conclusions, the identification of major intermediates have been carried out.

Electronic Structure of Iron Isoporphyrin and Iron Porphodimethene Derivatives. The limited available data do not give definitive information regarding the oxidation state and spin state of iron isoporphyrin and iron porphodimethene or their axial ligation. Likely oxidation states for all reaction products are Fe^{III} and Fe^{IV}. Available ligands are perchlorate, chloride, hexachloroantimonate, water, and pyridine. Since two

(53) Dolphin, D.; Felton, R. H.; Borg, D. C.; Fajer, J. *J. Am. Chem. Soc.* **1970**, *92*, 743.
(54) Guzinski, J. A.; Felton, R. H. *J. Chem. Soc., Chem. Commun.* **1973**, 715.
(55) Hinman, A. S.; Pavelich, B. J.; Kondo, A. E.; Pons, S. *J. Electroanal. Chem.* **1987**, *234*, 145.
(56) Balch, A. L.; Latos-Grażyński, L.; Noll, B. C.; Olmstead, M. M.; Zovinka, E. *Inorg. Chem.* **1992**, *31*, 1148.
(57) Johnson, A. W.; Winter, M. *Chem. Ind.* **1975**, 351.
(58) Dolphin, D. *J. Heterocycl. Chem.* **1970**, *7*, 275.
(59) (a) Shimidzu, T.; Segawa, H.; Iyoda, T.; Honda, K. *J. Chem. Soc., Faraday Trans. 2* **1987**, *83*, 2191. (b) Shimidzu, T.; Iyoda, T.; Segawa, H.; Honda, K. *Nouv. J. Chim.* **1986**, *10*, 213. (c) Richoux, M.; Neta, P.; Christensen, P. A.; Harriman, A. *J. Chem. Soc., Faraday Trans. 2* **1986**, *82*, 235.
(60) (a) Buchler, J. W.; Lay, K. M.; Lee, Y. J.; Scheidt, R. W. *Angew. Chem., Int. Ed. Engl.* **1982**, *21*, 432. (b) Botulinski, A.; Buchler, J. W.; Abbes, N. E.; Scheidt, W. R. *Liebigs Ann. Chem.* **1987**, 305. (c) Botulinski, A.; Buchler, J. W.; Wicholas, M. *Inorg. Chem.* **1987**, *26*, 1540. (d) Botulinski, A.; Buchler, J. W.; Lee, Y.; Scheidt, R. W.; Wicholas, M. *Inorg. Chem.* **1988**, *27*, 927. (e) Botulinski, A.; Buchler, J. W.; Lay, K. L.; Ensling, J.; Twilfer, H.; Billecke, J.; Leuken, H.; Tonn, B. *Adv. Chem. Ser.* **1982**, *No. 201*, 253.
(61) Fontecave, M.; Battioni, J. P.; Mansuy, D. *J. Am. Chem. Soc.* **1984**, *106*, 5212.

different ligands can be coordinated and the two axial coordinating sites are not equivalent, one can expect a large number of species to form for any given macrocyclic structure. On the combination of axial ligands the following spin states can be present for Fe^{III}: $S = {}^1/_2$, $S = {}^3/_2$, $S = {}^5/_2$, the quantum or thermal mixture $S = {}^5/_2/S = {}^3/_2$, and $S = {}^5/_2/S = {}^1/_2$.[40,42,60,62] In the case of Fe^{IV} the intermediate spin state $S = 1$ is expected.[22,31] Contrary to iron porphyrins, including the β-substituted iron porphyrins, the number of available spectroscopical models for meso-substituted paramagnetic metallotetraphenylporphyrins is rather restricted.

The pyrrole positions of the high-spin iron(III) isoporphyrin, obtained from iron(III) tetrakis(4-methoxyphenyl)porphyrin, are 104.6 ppm and 123.1 ppm (−70 °C).[40] Addition of cyanide converts this high-spin form into the low-spin derivatives with pyrrole resonances centered at a typical position for $[(TPP)Fe^{III}(CN)_2]^-$.[63] Four pyrrole resonances in the −10 to −30 ppm region were assigned to chromium(III) isoporphyrin ($S = {}^3/_2$).[56]

Buchler *et al.* presented an analysis of the ^1H NMR spectra of the high-spin iron(III) porphodimethene systems derived from OEP.[60] All the data collected up to now support a thesis that a general pattern of electronic structure−pyrrole resonance positions determined for paramagnetic metalloporphyrins[42] should be valid to some extent also for meso-substituted products. We have to take into account that the pure $S = {}^3/_2$ spin state produces a large upfield shift of the pyrrole resonances due to the presence of two unpaired electrons in the e_g metal ion orbitals.[62] However, a large upfield shift is also observed for iron(IV) porphyrins[22,31] and ruthenium(IV) porphyrins (d^4, $S = 1$).[52b] The smaller shift of the iron(III) low-spin species reflects the fact that only one e_g electron is available. On the basis of this conclusion and in view of the characteristic temperature dependencies of paramagnetic shifts, we have to consider two possible electronic states for species with pyrrole resonances located at high fields (−40 to −60 ppm at −70 °C), i.e., Fe^{III}, $S = {}^3/_2$, and/or Fe^{IV}, $S = 1$. We would like to point out that four pyrrole resonance, high-field-shifted species are formed in the presence of an excess of oxidizing agent with **1**-1 or **1**-2. The originally formed Fe^{III} complex can be oxidized to an Fe^{IV} complex in the step following the substitution by pyridine. The spectral parameters and temperature dependence suggest the following electronic states for two other forms: **4**-1, $S = {}^5/_2$; **4**-2, $S = {}^5/_2$ with some admixture of $S = {}^3/_2$ or $S = {}^1/_2$; **4**-3, $S = {}^1/_2$ with some admixture of $S = {}^5/_2$. The **4**-2 and **4**-3 species seem to present the extreme cases of $S = {}^5/_2 - S = {}^1/_2$ thermal equilibrium. In particular, the pyrrole resonance positions and relatively large line width of **4**-3 suggest an admixed spin state which contains a considerable fraction of the high-spin component.

Mechanistic Consideration. The plausible mechanisms for the formation of **2**−**4** include nucleophilic attack at the β- or *meso*-positions with a contribution from σ-intermediates. The overall stoichiometry is shown in the following equations:

$$2[(TPP^{\bullet})Fe^{III}]^{2+} + 2py \rightarrow [(\beta\text{-py-TPP})Fe^{III}]^{2+} + [(TPP)Fe^{III}]^{+} + pyH^{+} \quad (4)$$

$$2[(TPP^{\bullet})Fe^{III}]^{2+} + py \rightarrow [(meso\text{-py-TPP})Fe^{III}]^{3+} + [(TPP)Fe^{III}]^{+} \quad (5)$$

$$[(meso\text{-py-TPP})Fe^{III}]^{3+} + py \rightarrow [(di\text{-}(meso\text{-py})\text{-TPP})Fe^{III}]^{3+} \quad (6)$$

Mechanisms previously proposed for reactions of metalloporphyrin cation radicals or aromatic radicals with nucleophiles have been considered.[33-41,49,53-55,64-66]

Three different pathways should be taken into account: I. The iron porphyrin cation radical is attacked by a nucleophile at the meso position to give an adduct that is still a radical. Subsequent one-electron oxidation and/or a proton dissociation gives the expected β-(meso)-substitution product. II. The reaction proceeds via a dication formed by disproportionation of the cation radical. The dication reacts rapidly with nucleophiles. III. An iron porphyrin radical couples with a radical that was formed by one electron oxidation of the base (pyridine).

Route III, although considered by us previously for β-NO_2 or β-PPh_3 substitution in the case of easily oxidizable nucleophiles,[41] is not important in the case of pyridine substitution. The oxidation of pyridine to give the corresponding radical requires much a higher oxidation potential than that achievable by **1**. Pyridine is electrochemically inert between −2 and 2 V versus Ag/AgCl.[67] At the present stage, none of the plausible σ-intermediates could be directly identified by means of the methodology applied in the paper. In particular there is no direct spectroscopic evidence for the formation of $\{[(\beta\text{-py-TPP}^{\bullet})Fe^{III}]^{2+}\}$, $\{[(TPP)Fe^{III}]^{3+}\}$, the $\{[(\beta\text{-py-TPP})]Fe^{III}]^{3+}\}$ σ-intermediate, or $\{[(meso\text{-py-TPP}^{\bullet})Fe^{III}]^{2+}\}$ in the reaction mixture; the precedence of one-electron oxidation or pyridine addition could not be assigned.

The formation of the meso-substituted species **3** and **4** is of special interest. Formally, these are oxidized by two electrons with respect to iron(III) porphyrins. They represent a new form of highly oxidized, highly positively charged iron porphyrin related species.

The formation of the isoporphyrin **3** has been confirmed only by the characteristic four resonance pattern in the low-temperature ^1H NMR spectrum. Isoporphyrins are cationic and are expected to undergo further nucleophilic attack at the meso position opposite to one already bearing a pyridinium group.[33d,34c,64] The product of the second nucleophilic substitution was demonstrated to be iron(III) 5,15-dipyridiniumyltetraphenylporphodimethene. The macrocycles bear two positive charges at its periphery.

Porphodimethenes were obtained by reductive alkylation of metallooctaethylporphyrins[60] and iron(II) tetraphenylporphyrin.[61] Only selected examples were demonstrated where the reductive addition to the oxidized porphyrin resulted in the porphodimethene macrocycles, *i.e.* 5,15-dihydroxytetraphenylporphodimethene and dimethoxyporphodimethene.[57-59] Introduction of a pyridinium substituent at the meso positions resulted in rather crowded arrangement which seems quite unusual. However a similar structural fragment has been encountered in

(62) (a) Rodgers, K. R.; Goff, H. M. *J. Am. Chem. Soc.* **1987**, *109*, 611. (b) Balch, A. L.; Cheng, R.-J.; La Mar, G. N.; Latos-Grażyński, L. *Inorg. Chem.* **1985**, *24*, 2651. (c) Toney, G. E.; terHaar, Savrin, J. E.; Gold, A.; Hatfield, W. E.; Sangaiah, R. *Inorg. Chem.* **1984**, *23*, 2561. (d) Toney, G. E.; Gold, A.; Savrin, J. E.; terHaar, L. W.; Sangaiah, R.; Hatfield, W. E. *Inorg. Chem.* **1984**, *23*, 4350.

(63) Balch, A. L.; Latos-Grażyński, L.; Phillips, S. Unpublished results.

(64) Smith, K. M.; Barnett, G. H.; Evans, B.; Martynenko, Z. *J. Am. Chem. Soc.* **1979**, *101*, 5953.

(65) (a) Sankararaman, S.; Haney, A. W.; Kochi, J. K. *J. Am. Chem. Soc.* **1987**, *109*, 5235. (b) Masnovi, J. M.; Sankararaman, S.; Kochi, J. K. *J. Am. Chem. Soc.* **1989**, *111*, 2263.

(66) Chmielewski, P.; Latos-Grażyński, L.; Rachlewicz, K. *Magn. Reson.* **1993**, *31*, 547.

(67) (a) Eberson, L.; Nyberg, K. In *Advances In Physical Organic Chemistry*; Gold, V., Bethell, D., Eds.; Academic Press: London, 1976; Vol. 12, p 110. (b) Kadish, K. M.; Rhodes, R. K. *Inorg. Chem.* **1981**, *20*, 2961. (c) Kadish, K. M.; Shiue, L. R. *Inorg. Chem.* **1982**, *21*, 3623.

products of anodic processes which involved pyridine and 9,10-diphenylanthracene or tris(p-methoxyphenyl)ethylene.[68,69]

Conclusions

As part of a series of studies to understand the reactivity of iron porphyrin π-cation radicals, we have investigated their reactivity toward an electrochemically inert nucleophile—pyridine. The cation radical plays a dual role in the system. It acts as an electrophilic substrate for the reaction and as a one-electron oxidizing reagent. We have established that iron porphyrin cation radicals form β- and *meso*-substituted species that are analogs of the isoporphyrin and porphodimethene macrocycles. Their formation has been demonstrated by low-temperature NMR investigations. It is apparent that characteristic patterns of pyrrole resonances, i.e. seven for the β-substituted form, four for the isoporphyrin, and two for the porphodimethene iron complexes, can be used to detect the mode of structural modification. The reaction mechanism seems to be analogous to that elucidated for metalloporphyrin cation radicals for diamagnetic metal ions although our experiments provide the first direct evidence for the existence of such *meso*-substituted intermediates in the reaction pathway. The coordination of pyridine to iron(III) porphyrin cation radical has been also found.

The characterization of β-pyridiniumyltetraphenylporphyrin, -isoporphyrin, or -porphodimethene as the reaction products of iron porphyrin cation radical with pyridine suggests that any oxidation with iron porphyrin catalyst in the presence of pyridine may form such products. Pyridine may contribute to the reaction mechanism not only as a robust ligand which modifies the metal center activity but in addition as the macrocycle modifying reagent.

Formally, the iron(III) isoporphyrin and iron(III) porphodimethene are oxidized by two electrons with respect to iron(III) porphyrins. Potential nucleophiles such as histidyl or amino residues in hemoprotein are natural candidates for β- or *meso*-substitution of porphyrin macrocycle, and we suggest that the formation of isoporphyrin and/or porphodimethene species may be essential in the reactions of heme—protein cross-linking.

Experimental Section

All solvents were purified by standard procedures. Pyridine and 2,4,6-collidine were dried and distilled over KOH directly before use. Tetraphenylporphyrin ($TPPH_2$)[70] and $TPPH_2$-d_8-deuterated at β-pyrrole positions[71] were prepared using reported methods. Insertion of the iron and zinc ions into these porphyrins followed known routes.[72] The low-spin iron(III) porphyrins were obtained by addition of the appropriate ligand to a 2 mM solution of the complex. Pyridine-d_5 and 1-methylimidazole were used as received from Aldrich. Deuterated solvents [$CDCl_3$ (Glaser AG), CD_2Cl_2 and C_7D_8 (Aldrich)] were used as received in the ^1H NMR titrations of (β-py-TPP)$Fe^{III}Cl_2$ and related species with pyridine and 1-methylimidazole. Deuterated reagents used in the reactivity studies of iron porphyrin cation radicals were purified directly before experiments (CD_2Cl_2, distillation from CaH_2; C_5D_5N, distillation from KOH).

(TPP•)$Fe^{III}(ClO_4)_2$ and [(TPP•)$Fe^{III}Cl$][$SbCl_6$] were synthesized according to described procedures.[73] One-electron reduction of cation radicals (**1**-1) and (**1**-2) with KI resulted solely in a recovery of iron(III) tetraphenylporphyrin derivatives.

β-py-$TPPH_2Cl$ (β-py-d_5-$TPPH_2$)Cl was synthesized by the procedure described by Shine et al.[35] in the reaction of (TPP•)$Zn(ClO_4)$ with pyridine (pyridine-d_5). Electrochemical synthesis was also used and gave an identical product.[36]

{[(β-py-TPP)Fe^{III}]$_2$O}$(ClO_4)_2$. Method I. (TPP•)$Fe^{III}(ClO_4)_2$ (300 mg) was dissolved in dichloromethane (200 mL). The solution was stirred while dry pyridine (1.5 mL) in dichloromethane (20 mL) was added dropwise. After 1 h the solution was evaporated to dryness on a rotatory evaporator. The residue was dissolved in dichloromethane, and the solution was chromatographed on a column of neutral alumina. Elution with dichloromethane gave [(TPP)Fe]$_2$O. Elution with 5% v/v of ethanol in dichloromethane gave two iron porphyrin fractions. The second one was identified as {[(β-py-TPP)Fe^{III}]$_2$O}$(ClO_4)_2$ by means of ^1H NMR spectroscopy. Recrystallization from dichloromethane/hexane gave 120 mg of the green powder (20% yield).

Method II. A modification of the acetate method[50] was applied. Solid $Fe^{II}Cl_2$·$4H_2O$ (50 mg), CH_3COOK (1.5 g), and β-py-$TPPH_2Cl$ (50 mg) were added to glacial acetic acid (50 mL). The solution was heated under reflux for 1 h under nitrogen. The iron porphyrin products were extracted into chloroform. This solution was washed with water (to remove acetic acid), evaporated, and chromatographed as described above. UV/vis (CH_2Cl_2): λ_{max}/nm (log ε) = 324 (4.66), 416 sh (5.00), 516 (4.43), 582 (4.26), 619 sh (4.00).

(β-py-TPP)$Fe^{III}Cl_2$. Hydrogen chloride in dichloromethane was added to a solution of {[(β-py-TPP)Fe^{III}]$_2$O}$(ClO_4)_2$ in dichloromethane (the color changed from green to red). The solution was evaporated to dryness. The resulting solid was recrystallized from dichloromethane/hexane. Anal. Calcd for $C_{49}H_{32}N_5Cl_2Fe$: C, 71.99; H, 3.95; N, 8.57. Found: C, 71.67; H, 3.80; N, 8.48. UV/vis (CH_2Cl_2): λ_{max}/nm (log ε) = 370 (4.61), 424 (4.80), 513 (3.99), 583 sh (3.66), 693 (3.32).

Samples of the bromo and iodo derivatives of β-substituted iron(III) prophyrins were obtained from the corresponding (μ-oxo)diiron compounds in an analogous way. Anal. Calcd for $C_{49}H_{32}N_5Br_2Fe^{III}/_2CH_2Cl_2$: C, 62.65; H, 3.5; N, 7.38. Found: C, 63.06; H, 3.82; N, 7.48. UV/vis (CH_2Cl_2): λ_{max}/nm (log ε) = 388 (4.76), 428 (4.85), 519 (4.12), 584 sh (3.76), 703 (3.42).

Low-Temperature Reactivity Studies. The required number of pyridine equivalents (approximately 1×10^{-3} nM in CD_2Cl_2) were added by microliter syringe to a sample of the iron(III) porphyrin cation radical **1**-1 or **1**-2 at −80 °C in an NMR tube that was sealed with a septum cap. The sample was shaken in a cold bath and transferred to the precooled NMR probe to follow the progress of the reaction.

Instrumentation. ^1H NMR spectra were recorded on a Bruker AMX spectrometer operating in the quadrature mode at 300 MHz. A typical spectrum was collected over a 45 000 Hz spectral window with 16 K data points with 500−5000 transients for the experiment and a 50 ms prepulse delay. The free induction decay (FID) was apodized using exponential multiplication depending on the natural line width. This induced 5−50 Hz broadening. The residual ^1H NMR spectra of the deuterated solvents were used as a secondary references.

The ^2H NMR spectra were collected using a Bruker AMX instrument operating at 46.1 MHz. A spectral width of 20 kHz was typical and 16 K points was used. A pulse delay of 50 ms was used. The signal to noise ratio was improved as in proton spectra. The residual ^2H NMR resonance of the solvents was used as a secondary reference.

The COSY spectrum was obtained after collecting a standard 1D reference spectrum. The 2D spectrum was collected by use of 1024 points in t_2 over the desired bandwith (to include all desired peaks) with 258 t_1 blocks and 1024 scans per block. All experiments included four dummy scans prior to the collection of the first block.

Absorption spectra were recorded on a Specord M-42 spectrophotometer. EPR spectra were recorded at the X-band on the SE/X Radiopan spectrometer.

Acknowledgment. The financial support of the State Committee for Scientific Research KBN (Grant 2 2651 92 03) is kindly acknowledged.

IC930771M

(68) (a) Parker, D. V.; Eberson, L. *J. Chem. Soc., Chem. Commun.* **1969**, 451. (b) Manning, G.; Parker, V. D.; Adams, R. N. *J. Chem. Soc.* **1969**, 4584.
(69) (a) Blount, H. N. *J. Electroanal. Chem.* **1973**, *42*, 271. (b) Blount, H. N. *J. Electroanal. Chem.* **1974**, *54*, 305.
(70) Lindsey, J. S.; Schreiman, I. C.; Hsu, H. C.; Kearney, P. C.; Marguerettaz, A. M. *J. Org. Chem.* **1987**, *52*, 827.
(71) Boersma, A. D.; Goff, H. M. *Inorg. Chem.* **1982**, *21*, 581.
(72) Adler, A. D.; Longo, F. R.; Kampas, F.; Kim, J. *J. Inorg. Nucl. Chem.* **1970**, *32*, 2443.
(73) Gans, P.; Buisson, G.; Duée, E.; Marchon, J.-C.; Erler, B. S.; Scholz, W. F.; Reed, C. A. *J. Am. Chem. Soc.* **1986**, *108*, 1223.